Energy Equip. Sys./ Vol. 11/No. 3/September 2023/ 353-369

ENERGY EQUIPSYS

Energy Equipment and Systems
http://energyequipsys.ut.ac.ir
www.energyequipsys.com

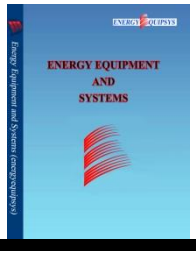

Techno-economic investigations of a new cogeneration energy system for hydrogen, ammonia, and power generation

Authors

Behzad Farhang[a]
Hadi Ghaebi[a*]
Nader Javani[b]

[a] Department of Mechanical Engineering, University of Mohaghegh Ardabili, P.O. Box 179, Ardabil, Iran

[b] Faculty of Mechanical Engineering, Yildiz Technical University, 34349, Istanbul, Turkey

ABSTRACT

This study aims to develop, and examine a cogeneration system for electric power, hydrogen, and ammonia production. A modified Rankine cycle is configured to supply power. An electrolyze unit and an ammonia synthesis reactor are used to provide hydrogen and ammonia. The system is investigated from technical and economic aspects. The inquiry outcomes disclose that the reaction pressure and hydrogen to nitrogen molar ratio have mainly affected the ammonia production rate increment. The system energy and exergy efficiencies as well as the total unit cost of the product are at about 50.47 %, 51.41 %, and 638.3 $/GJ, respectively. The results show that the exergy destruction rate of the system is 89.797 MW. Moreover, 6.438 kg/h of hydrogen and 6.528 kg/s of ammonia are attainable. The sweeping sensitivity investigation on the economic aspect reveals that the reaction pressure, input hydrogen molar ratio, and hydrogen to nitrogen molar ratio have a positive effect on the sum unit cost of the product's decrement. Finally, the thermodynamic sensitivity examination outcomes affirm that altering reaction temperature leads to technical inefficiencies in the proposed cogeneration system.

Article history:

Received : 10 May 2023
Accepted : 28 May 2023

Keywords: Exergoeconomic Analysis, Hydrogen, Thermodynamic Analysis, Ammonia, Cogeneration Plant, Exergy Efficiency.

1. Introduction

Considering the current energy consumption patterns indicates an increasing trend for the near future. This increase is expected to be 44% in the upcoming years. A switch to alternative fuels to avoid the unfavorable outcomes of fossil fuels is therefore unavoidable [1, 2].

In cogeneration energy systems by increasing the number of useful outputs, the system would have higher efficiency and consequently improved performance [3]. Recently, several endeavors have been earmarked for the new layout of cogeneration energy systems for the production of useful commodities including hydrogen and ammonia [4-7].

Ghaebi et al.[8] reviewed a state-of-the-art design of a solid oxide fuel cell (SOFC)/gas turbine integrated cycle plant with a biogas reforming cycle for hydrogen and electric power cogeneration. A sensitivity study has been conducted for the consequence of various variables on the net electric power, energy and

* Corresponding author: Hadi Ghaebi
Department of Mechanical Engineering, University of Mohaghegh Ardabili, P.O. Box 179, Ardabil, Iran
Email: hghaebi@uma.ac.ir

exergy efficiencies, rate of destructed exergy, and the sum unit cost of products (SUCP) of the entire plant. The outcomes showed that the energy and exergy efficacies of the suggested incorporated plant had increased compared to the SOFC/gas turbine system by 23.3% and 28.2%, approximately. The obtained net electric power and hydrogen generation rates are about 2726 kW and 0.075 kg/s, respectively. Hashemian et al. [9] combined a PEM unit with a solar/biomass-powered cogeneration energy system to generate hydrogen and power. The developed system was evaluated from advanced thermodynamic and advanced thermoeconomic aspects. As their results showed, the solar thermal unit had the most feasibility to diminish the total destructed exergy. Chitgar and Emadi [10] developed a cogeneration system to guarantee the request for electricity and hydrogen. Moreover, after completing an exergoeconomic investigation of the aimed system, the optimum points of performance for the plant were determined. The conclusions pictured that the plant could supply 2.5 MW of electricity and 1.8 kg/h of hydrogen. A new cogeneration energy system was studied by Musharavati et al. [11]. Thermodynamic-based modeling was conceived and exergetic appraisals were employed to assess the system. Results revealed that the inefficient component of the plant from the exergy destruction point of view was linked to the equipment to receive input energy. Jabari et al. [12] conducted a study on the stand-alone cogeneration plant with power production options and scrutinized its implementation under various reference air temperatures and different load levels. This new cogeneration system is capable of generating 5.8 MW of power for large industrial sectors with a low efficiency of 37%. Substituting natural gas with biofuels in this offered plant resulted in emissions mitigation. A new electricity and hydrogen production plant was offered by Soleymani et al. [13]. The submitted plant examined two aspects of thermodynamics and thermoeconomics. Also, the consequence of several critical variables on the major interpretation criteria was reckoned. The energy efficiency of the integrated plant grew from about 52.3% to 64.5%. Moreover, the exergy efficiency improved from 50.5% to 64.6%. Cao et al. [14] evaluated and compared a cogeneration system with power and hydrogen generation options with thermodynamic and thermoeconomic characteristics. They reported that the electrolyzer-absorption power cycle passed the most satisfactory implementation. Besides, a sweeping parametric evaluation was brought out on the plant to investigate the influence of the critical parameters on the function of the system. Sattari Sadat [15] introduced a system for hydrogen and electric power generation. Thermodynamic and thermoeconomic analyses were carried out. The energy and exergy efficacies were calculated as 79.5% and 33.9%. Moreover, the SUCP of the plant may be minimized with gas turbine output pressure. Meantime, a thorough sensitivity examination of the plant was conducted, showing that the proffered cogeneration system's exergetic efficiency may be maximized with the compression ratio. Yilmaz and Ozturk [16] submitted a novel integrated system and developed it for hydrogen and ammonia production. The developed plant was scrutinized thermodynamically including energy and exergy efficacies. The total energy and exergy efficacies of that developed system were at about 61.04% and 57.13%, respectively. Parametric research was accomplished to specify the influence of individual parameters on the plant's execution. An exergy analysis for the industrial-scale of the ammonia generation plant is also studied elsewhere. Exergy efficiency descriptions for the different elements and unit processes were calculated. The vital connection between irreversibilities and interpretation of the reactor was emphasized.

There are a few studies in the literature focusing on the thermodynamic aspect of the systems with ammonia production options, without a comprehensive exergoeconomic studies for cogeneration with ammonia production. In this work, an original cogeneration energy system is considered in which a PEM unit, a Kalina cycle system, and an ammonia synthesis unit are integrated for hydrogen, power, and ammonia production. The offered plant is scrutinized comprehensively from multi-aspects. In addition, a robust sensitivity analysis has been conducted. The main objectives and the novelties of the current study are as follows:

- To propose a new cogeneration energy system for hydrogen, ammonia, and power generation, using a PEM and synthesis reactor incorporated unit.
- To involve a Kalina cycle system (for power production), an ammonia synthesis reactor (for ammonia production), and a PEM unit (for hydrogen production) for designing purposes
- To scrutinize the plant from thermodynamic and thermoeconomic views
- To conduct a comprehensive sensitivity evaluation for the target plant

Nomenclature

Symbols

A	Area
e	Specific exergy, kJ/kg
$\dot{E}$	Exergy rate, kW
F	Faraday constant
G	Gibbs free energy
h	Enthalpy, $kJ.kg^{-1}$
Ir	Interest rate, %
J^{ref}	Pre-exponential factor, A/m^2
J_0	Exchange current density, A/m^2
J	Current Density, A/m^2
L	Membrane thickness, m
$\dot{m}$	Mass flow rate, kg/s
n	Mole/Lifetime
P	Pressure, bar
Q	Heat
R	Universal gas constant, J/mol.K
SUCP	Sum unit cost of the product
s	Entropy, $kJ.kg^{-1}.K^{-1}$
T	Temperature, K
y	Mole fraction
Z	Elements cost, $
$\dot{Z}$	Cost rate of elemets, $/s

Acronyms

cond	Condenser
CRF	The factor of capital recovery
EES	Engineering equation solver
HE	Heat exchanger
H_2	Hydrogen
H_2O	Water
LHV	Low heating value, kJ/kg
N	System yearly work hours
NH_3	Ammonia
pr	Product
read	Reactor
th	Thermal
tot	Total
tur	Turbine

Subscripts and superscripts

0	Reference condition
ch	Chemical
CI	Capital investment
com	Compressor
D	Destruction
fu	Fuel
is	Isentropic
LMTD	Logarithmic mean temperature difference
mem	Membrane
mix	mixer
OM	Operating and maintenance
ph	Physical
Ẇ	Power, kW
U	Coefficient of heat transfer, kW/m^2K

Greek symbols

η	Efficiency
φ	Maintenance factor
λ	Water content
σ	proton conductivity in PEM, 1/ Ω m

2. System Description

The proposed cogeneration system with its components are illustrated in Fig. 1.. The plant incorporates a Rankine cycle, an ammonia synthesis unit, and a PEM electrolyzer for electricity, ammonia, and hydrogen production.

2.1 Kalina cycle system (KCS)

This unit enclosed turbine, regenerator, separator, condenser, electric generator, and pump units. A part of the output water vapor from the ammonia synthesis reactor infiltrates the separator and then to the turbine, where a portion of the operating fluid is gained at a lower pressure (point 10). In the output of the turbine, the operating fluid goes to the mixer1 and then enters the condenser at relatively increased temperatures. The liquefied working fluid in the condenser (point 2) is pumped to the increased pressure of a regenerator via pump (point 3). Finally, the operating fluid is returned to the ammonia synthesis reactor (point 4) and on the other side, power generated via the turbine ends the electricity generation process. Meanwhile, a percentage of the supplied electricity by the turbine is utilized straightly (DC electricity) and another share is employed by the kit in the electrolyzer unit.

2.2 Hydrogen production unit

In the unit that is linked to the ammonia synthesis reactor, water is split by a PEM electrolyzer into hydrogen and oxygen (point 29). The electrolyzer is functioned by the power supplied by the plant. The extra provided hydrogen is stored in the hydrogen storage tanks (point 28).

2.3 Ammonia synthesis reactor

In mixer2, the provided hydrogen (point 13) combines with nitrogen (point 14) and joins the reactor of ammonia synthesis (point 22) following crossing through four compressors and three intercoolers. The pressure of the initial mixture in the compressor1 increases up to 20 bar (points 15 and 16). Then the mixture in intercooler 1 gives part of its heat to the reactor and after that, it is cooled down to the ambient temperature by the cooling water. This process continues with the other compressors and intercoolers (points 17 to 22). At point 22, the mixture, which has experienced an increase in pressure in each stage, finally reaches the pressure of the ammonia synthesis reactor. The outlet flow from the ammonia synthesis reactor penetrates the condenser and the ammonia, which is diverged from nitrogen and hydrogen (point 25), is made (point 24).

The thermodynamic simulation Includes energy and exergy studies, based on the first law and second law of thermodynamics, respectively. Furthermore, the exergoeconomic study is conducted to include economic aspects. To assure a reliable modeling of the offered cogeneration energy systems, EES [17] is applied as a robust thermodynamic modeling software. Following assumptions are considered in the modeling process [18-20]:

- The steady-state limitations are accepted in the modeling of the cogeneration system.
- An elimination is thought for any pressure drop into the equipment like pipelines, heat exchangers, and so on.
- The saturated vapor has been transferred to the fluid exiting the condenser.
- Valves are considered as isenthalpic processes.
- Kinetic and potential energy and exergy modifications are neglected.

Other data for the modeling process are listed in Table 1.

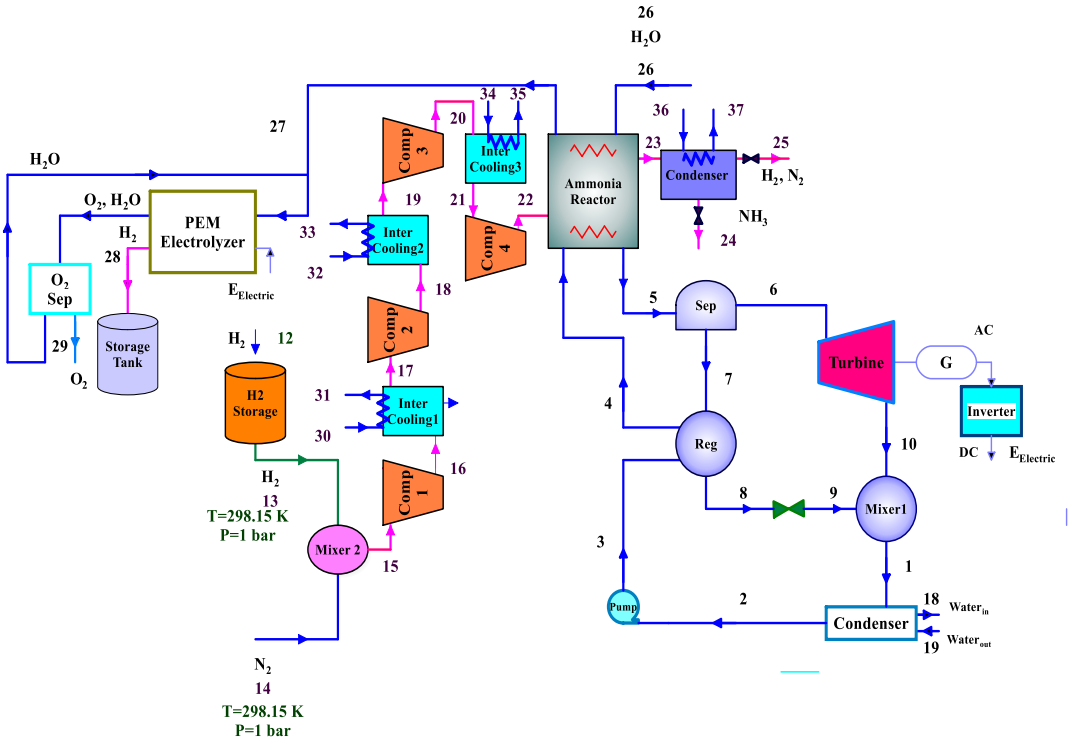

Fig. 1. Schematic diagram of the cogeneration system.

Table 1. The required input parameters for simulation of the proposed cogeneration systems [21-24]

Reference temperature, T_0(K)	298.15	Oxygen pressure, P_{O_2} (kPa)	101
Reference pressure, P_0(bar)	1.01	Hydrogen pressure, P_{H_2} (kPa)	101
Turbine inlet temperature, $T_{in,TUR}$ (^{o}C)	140	PEM Temperature, T_{PEM} (^{o}C)	80
Condensing final temperature, $T_{COND/ABS}$ (^{o}C)	50	Anode activation energy, $E_{act,a}$(kJ/mol)	76
NH_3H_2O fraction at vapor generator inlet X_3 (%)	36	Cathode activation energy, $E_{act,c}$(kJ/mol)	18
Hydrogen to nitrogen molar ratio, C_{HN}	3	Membrane anode surface water, λ_a	14
Hydrogen and nitrogen inlet pressure, P_{in}(bar)	1.013	Membrane cathode surface water, λ_c	10
Hydrogen and nitrogen inlet temperature, T_{in}(K)	298.15	Membrane thickness, D (μm)	100
Ammonia synthesis reaction pressure, P_{Reac} (bar)	100	Anode pre-expotential factor , J_a^{ref}	1.7×10^5
Ammonia synthesis reaction temperature, T_{Reac} (K)	548	Cathode pre-expotential factor, J_c^{ref}	4.6×10^3
Turbines, pumps and compressors isentropic efficiency, η_{is} (%)	85	Faraday constant, F (C/mol)	96486

The first law of thermodynamics is used for every component of the plant. The mass and energy balance equations for the steady-state situations are given by [25]

$$\sum \dot{m}_{inlet,k} = \sum \dot{m}_{outlet,k}, \tag{1}$$

$$\dot{Q}_k + \sum \dot{m}_{inlet,k} h_{inlet,k} = \sum \dot{m}_{outlet,k} h_{outlet,k} + \sum \dot{W}_k . \tag{2}$$

Here, h_k, $\dot{W}_k$, and $\dot{Q}_k$ show the enthalpy, power, and heat transfer rate, respectively.

In order to have a better idea for the exergy loss of the components and to improve the second law efficiency, the exergy destruction rates are also calculated using

$$\dot{E}_{ph,i} = \dot{m}\left(h_i - h_0 - T_0\left(s_i - s_0\right)\right), \tag{3}$$

$$\dot{E}_{ch,i} = \dot{m}\left(\sum_i y_i \bar{e}_i^{ch,O} + \bar{R}T_O \sum_i y_i ln y_i\right)_i . \tag{4}$$

Here, $\dot{E}_{ch,i}$ and $\dot{E}_{ph,i}$ are chemical and physical exergies, each. Also, 0, s, and $\bar{e}_i^{ch,O}$ show the reference state, entropy, and standard chemical exergy of the mixture. The quantity of the standard chemical exergy for the different mixtures are found in the literature [26]. Thus, the total rate of exergy may be written as

$$\dot{E}_{tot,i} = \dot{E}_{ph,i} + \dot{E}_{ch,i} \tag{5}$$

Exergy destruction rate ($\dot{E}_{D,k}$), therefore, can be written as

$$\dot{E}_{D,k} = \dot{E}_{fu,k} - \dot{E}_{pr,k} \tag{6}$$

where $\dot{E}_{fu,k}$ and $\dot{E}_{pr,k}$ denote exergetic rates of the fuel and product for the kth element of the cogeneration energy system, sequentially. Moreover, the destructed exergy rate may be calculated via

$$\dot{E}_{D,k} = \sum_j \left(1 - \frac{T_0}{T_j}\right)\dot{Q}_j - \dot{W}_{CV} + \sum_k \dot{E}_{k,in} - \sum_k \dot{E}_{k,out} \tag{7}$$

In addition, the exergy rates of the heat transfer and work can be written as

$$\dot{E}_Q = \dot{Q}_j\left(1 - \frac{T_0}{T_j}\right) \tag{8}$$

$$\dot{E}_W = \dot{W}_{cv} . \tag{9}$$

The energetic and exergetic balance details for all elements are given in Table 2.

Based on the logarithmic mean temperature difference ($\Delta T_{LMTD,k}$) and the overall coefficient of heat transfer (U_k) , the heat transfer area can be calculated using

$$A_k = \frac{\dot{Q}_k}{U_k \Delta T_{LMTD,k}}, \tag{10}$$

where

$$\Delta T_{LMTD} = \frac{\Delta T_A - \Delta T_B}{\ln \frac{\Delta T_A}{\Delta T_B}} \tag{11}$$

In addition, the overall heat transfer coefficient for all heat exchangers is listed in Table 3.

Table 2. Mass and energy balance equations applied to each component of the system

Component	Mass and energy balance equations	Exergy balance equation
KSC-Turbine	$\dot{W}_{\mathrm{KSC-TUR}} = \eta_{\mathrm{is}}\dot{m}_6(h_6 - h_{10\mathrm{s}})$	$\dot{E}_{D,\mathrm{KSC}-TUR} = (\dot{E}_6 - \dot{E}_{10}) - \dot{W}_{\mathrm{KSC-TUR}}$
Separator	$\dot{m}_5 = \dot{m}_6 + \dot{m}_7$, $\dot{m}_5X_5 = \dot{m}_6X_6 + \dot{m}_7X_7$	$\dot{E}_{D,SEP} = \dot{E}_5 - (\dot{E}_6 + \dot{E}_{10})$
Mixer 1	$\dot{m}_1 = \dot{m}_9 + \dot{m}_{10}$, $\dot{m}_1h_1 = \dot{m}_9h_9 + \dot{m}_{10}h_{10}$	$\dot{E}_{D,MIX1} = (\dot{E}_9 + \dot{E}_{10}) - \dot{E}_1$
Regenerator	$\dot{Q}_{KSC-REG}=\dot{m}_3(h_4 - h_3)$, $\dot{Q}_{KSC-REG} = \dot{m}_7(h_7 - h_8)$	$\dot{E}_{D,REG} = (\dot{E}_7 - \dot{E}_8) - (\dot{E}_4 - \dot{E}_3)$
Expansion Valve	$h_8 = h_9$	$\dot{E}_{D,EV} = \dot{E}_8 - \dot{E}_9$
Condenser	$\dot{Q}_{KSC-COND}=\dot{m}_1(h_1 - h_2)$, $\dot{Q}_{KSC-COND} = \dot{m}_{18}(h_{19} - h_{18})$	$\dot{E}_{D,COND} = (\dot{E}_1 - \dot{E}_2) - (\dot{E}_{19} - \dot{E}_{18})$
Pump	$\dot{W}_{\mathrm{PUM}} = \frac{\dot{m}_3(h_3 - h_{2\mathrm{s}})}{\eta_{\mathrm{is}}}$	$\dot{E}_{D,PUM} = \dot{W}_{\mathrm{PUM}} - (\dot{E}_3 - \dot{E}_2)$
Mixer 2	$\dot{m}_{15} = \dot{m}_{13} + \dot{m}_{14}$, $\dot{m}_{15}h_{15} = \dot{m}_{13}h_{13} + \dot{m}_{14}h_{14}$	$\dot{E}_{D,Mix2} = (\dot{E}_{13} + \dot{E}_{14}) - \dot{E}_{15}$
Compressor 1	$\dot{W}_{\mathrm{Com1}} = \frac{\dot{m}_{15}(h_{16\mathrm{s}} - h_{15})}{\eta_{\mathrm{is}}}$	$\dot{E}_{D,Com1} = \dot{W}_{\mathrm{Com1}} - (\dot{E}_{16} - \dot{E}_{15})$
Inter cooling 1	$\dot{Q}_{Int-cool1}=\dot{m}_{16}(h_{16} - h_{17})$, $\dot{Q}_{S-HE2} = \dot{m}_{37}(h_{37} - h_{38})$	$\dot{E}_{D,Int-Cool1} = (\dot{E}_{16} - \dot{E}_{17}) - (\dot{E}_{Q-Int1})$
Compressor 2	$\dot{W}_{\mathrm{Com2}} = \frac{\dot{m}_{17}(h_{18\mathrm{s}} - h_{17})}{\eta_{\mathrm{is}}}$	$\dot{E}_{D,Com2} = \dot{W}_{\mathrm{Com2}} - (\dot{E}_{18} - \dot{E}_{17})$
Inter cooling 2	$\dot{Q}_{Int-cool2}=\dot{m}_{18}(h_{18} - h_{19})$, $\dot{Q}_{S-HE2} = \dot{m}_{37}(h_{37} - h_{38})$	$\dot{E}_{D,Int-Cool2} = (\dot{E}_{18} - \dot{E}_{19}) - (\dot{E}_{Q-Int2})$
Compressor 3	$\dot{W}_{\mathrm{Com3}} = \frac{\dot{m}_{19}(h_{20\mathrm{s}} - h_{19})}{\eta_{\mathrm{is}}}$	$\dot{E}_{D,Com3} = \dot{W}_{\mathrm{Com3}} - (\dot{E}_{20} - \dot{E}_{19})$
Inter cooling 3	$\dot{Q}_{Int-cool3}=\dot{m}_{20}(h_{21} - h_{20})$, $\dot{Q}_{S-HE2} = \dot{m}_{37}(h_{37} - h_{38})$	$\dot{E}_{D,Int-Cool3} = (\dot{E}_{20} - \dot{E}_{21}) - (\dot{E}_{Q-Int3})$
Compressor 4	$\dot{W}_{\mathrm{Com4}} = \frac{\dot{m}_{21}(h_{22\mathrm{s}} - h_{21})}{\eta_{\mathrm{is}}}$	$\dot{E}_{D,Com4} = \dot{W}_{\mathrm{Com4}} - (\dot{E}_{22} - \dot{E}_{21})$
Ammonia Reactor	$\dot{Q}_{Reac}=\dot{m}_{22}(h_{22} - h_{23})$, $\dot{Q}_{Reac} = \dot{m}_5(h_5 - h_4)$	$\dot{E}_{D,Reac} = (\dot{E}_{22} - \dot{E}_{23}) - (\dot{E}_5 - \dot{E}_4)$
Condenser	$\dot{Q}_{Cond}=\dot{m}_{30}(h_{30} - h_{31})$, $\dot{Q}_{Cond} = \dot{m}_{46}(h_{47} - h_{46})$	$\dot{E}_{D,Cond} = (\dot{E}_{Q-Cond} + \dot{E}_{23}) - (\dot{E}_{24} + \dot{E}_{25})$
PEM-HE	$\dot{Q}_{PEM-HE}=\dot{m}_{14}(h_{27} - h_{26})$,	$\dot{E}_{D,PEM-HE} = (\dot{E}_{27} - \dot{E}_{26})$
PEM-Electrolyzer	See Appendix A	$\dot{E}_{D,\mathrm{PEM-Elec}} = \dot{E}_{PEM-Elec} - (\dot{E}_{16} + \dot{E}_{17} - \dot{E}_{15})$
PEM thermal efficiency	$\eta_{PEM-th} = \frac{\dot{m}_{PEM-H2}LHV_{\mathrm{H2}}}{\dot{W}_{Net} + \dot{Q}_{PEM-HE}}$	$\eta_{PEM-ex} = \frac{\dot{E}_{PEM-H2}}{\dot{W}_{Net} + \dot{E}_{PEM-HE}}$
Ammonia synthesis thermal efficiency	$\eta_{Syn-th} = \frac{\dot{m}_{NH3}LHV_{\mathrm{NH3}}}{\dot{m}_{H2}LHV_{\mathrm{H2}} + \dot{W}_{Com1234}}$	$\eta_{Syn-ex} = \frac{\dot{E}_{NH3}}{\dot{E}_{Syn-H2}}$
System efficiency	$\eta_{Sys-th} = \frac{\dot{m}_{NH3}LHV_{\mathrm{NH3}} + \dot{m}_{H2}LHV_{\mathrm{H2}} + \dot{W}_{Net}}{\dot{m}_{H2}LHV_{\mathrm{H2}} + \dot{W}_{Com1234}}$	$\eta_{Sys-ex} = \frac{\dot{E}_{NH3} + \dot{E}_{PEM-H2} + \dot{W}_{Net}}{\dot{E}_{Syn-H2} + \dot{W}_{Com1234}}$

Table 3. The overall heat transfer coefficient for all heat exchangers [27]

Component	$U\ (kW/m^2K)$
Regenerator	0.9
Condenser	1.1
Intercooler	1
Reactor	1.6
PEM heat exchanger	1

Finally, for the net electricity output ($\dot{W}_{net}$):

$$\dot{W}_{net} = \dot{W}_{TUR} - \dot{W}_{Pump} - \Sigma W_{comps} - \Sigma W_{intercoolers} \quad (12)$$

The exergoeconomic study is also used to investigate the economic investigation and conventional exergy simultaneously. In this case, the production costs of the plant are considered along with the produced exergy. The root of this study is the concurrent explanation of the cost balance (per exergy unit) relation for each system element. The balance of the cost rate relation of the element k is reported as [28]

$$\dot{C}_{q,k} + \sum \dot{C}_{in,k} + \dot{Z}_{tot}^{CI+OM} = \dot{C}_{w,k} + \sum \dot{C}_{out,k} \quad (13)$$

where $\dot{C}$ denote the cost rate and $\dot{Z}$ refers to the cost rate concerning capital investment and maintenance. The cost rate is given by [29, 30]

$$\dot{C} = c \times \dot{E} \quad (14)$$

where c shows the specific exergy cost in \$/GJ.

Cost rate of the exergy destruction is also defined as [31]

$$\dot{C}_D = c_F \times \dot{E}_{F,k} \quad (15)$$

where c_F shows the fuel cost. The total cost rate for the k[th] elements is defined as [32]

$$\dot{Z}_k^{CI+OM} = \dot{Z}_k^{CI} + \dot{Z}_k^{OM} \quad (16)$$

where

$$\dot{Z}^{CI+OM}{}_k = \frac{z_k \times \varphi \times CRF}{N} \quad (17)$$

Here, φ and N show the factor of maintenance and the plant annual working hours, which are 1.06 and 7000 hours, respectively. CRF is the capital recovery factor as

$$CRF = \frac{Ir(Ir+1)^n}{(1+Ir)^n - 1} \quad (18)$$

"Ir" and "n" represent the interest rate and the system lifetime, which are designated to be 0.12 and 20 years in the existing research. The cost relations for all elements of the cogeneration energy system are listed in Table 4.

Table 4. The cost equations applied to each component of the system [14, 33, 34]

Component	İnvestment cost	Cost balance	Auxilary relations
KSC-Turbine	$Z_{\mathrm{APC-TUR}} = 4405 * (\dot{W}_{\mathrm{TUR}})^{0.7}$	$\dot{C}_6 + \dot{Z}_{\mathrm{KSC-TUR}} = \dot{C}_{10} + \dot{C}_{\mathrm{KSC-TUR}}$	$c_6 = c_{10}$
Separator	$Z_{\mathrm{SEP}} = 0$	$\dot{C}_5 + \dot{Z}_{\mathrm{SEP}} = \dot{C}_7 + \dot{C}_6$	$c_6 = c_7$
Mixer	$Z_{\mathrm{MIX}} = 0$	$\dot{C}_9 + \dot{C}_{10} + \dot{Z}_{\mathrm{MIX}} = \dot{C}_1$	-
Regenerator	$Z_{\mathrm{REG}} = 130(\frac{A_{\mathrm{REG}}}{0.093})^{0.78}$	$\dot{C}_3 + \dot{C}_7 + \dot{Z}_{\mathrm{REG}} = \dot{C}_4 + \dot{C}_8$	$c_7 = c_8$
Expansion Valve	$Z_{\mathrm{EV}} = 114.5 * \dot{m}_4$	$\dot{C}_8 + \dot{Z}_{\mathrm{EV}} = \dot{C}_9$	-
Condenser1	$Z_{\mathrm{COND}} = 130(\frac{A_{\mathrm{COND1}}}{0.093})^{0.78}$	$\dot{C}_1 + \dot{C}_{18} + \dot{Z}_{\mathrm{COND}} = \dot{C}_2 + \dot{C}_{19}$	$c_1 = c_2$
Pump	$Z_{\mathrm{PUM}} = 3540(\dot{W}_{\mathrm{PUM}})^{0.71}$	$\dot{C}_2 + \dot{C}_{\mathrm{PUM}} + \dot{Z}_{\mathrm{PUM}} = \dot{C}_3$	$\frac{\dot{C}_{\mathrm{KSC-TUR}}}{\dot{W}_{\mathrm{KSC-TUR}}} = \frac{\dot{C}_{\mathrm{PUM}}}{\dot{W}_{\mathrm{PUM}}}$
Mixer 2	$Z_{\mathrm{Mix}} = 0$	$\dot{C}_{13} + \dot{C}_{14} + \dot{Z}_{\mathrm{Mix}} = \dot{C}_{15}$	-
Compressor 1	$Z_{\mathrm{Com1}} = 10167.5(\dot{W}_{\mathrm{Com1}})^{0.46}$	$\dot{C}_{15} + \dot{C}_{\mathrm{C1}} + \dot{Z}_{\mathrm{Com1}} = \dot{C}_{16}$	-
Inter cooling 1	$Z_{\mathrm{Int-cool1}} = 2143(A_{\mathrm{Int-cool1}})^{0.514}$	$\dot{C}_{30} + \dot{C}_{16} + \dot{Z}_{\mathrm{Int-cool1}} = \dot{C}_{31} + \dot{C}_{17}$	$c_{16} = c_{17}$
Compressor 2	$Z_{\mathrm{Com2}} = 10167.5(\dot{W}_{\mathrm{Com2}})^{0.46}$	$\dot{C}_{17} + \dot{C}_{\mathrm{C2}} + \dot{Z}_{\mathrm{Com2}} = \dot{C}_{18}$	-
Inter cooling 2	$Z_{\mathrm{Int-cool2}} = 2143(A_{\mathrm{Int-cool2}})^{0.514}$	$\dot{C}_{32} + \dot{C}_{18} + \dot{Z}_{\mathrm{Int-cool2}} = \dot{C}_{33} + \dot{C}_{19}$	$c_{18} = c_{19}$
Compressor 3	$Z_{\mathrm{Com3}} = 10167.5(\dot{W}_{\mathrm{Com3}})^{0.46}$	$\dot{C}_{19} + \dot{C}_{\mathrm{C3}} + \dot{Z}_{\mathrm{Com3}} = \dot{C}_{20}$	-
Inter cooling 3	$Z_{\mathrm{Int-cool3}} = 2143(A_{\mathrm{Int-cool3}})^{0.514}$	$\dot{C}_{34} + \dot{C}_{20} + \dot{Z}_{\mathrm{Int-cool3}} = \dot{C}_{35} + \dot{C}_{21}$	$c_{20} = c_{21}$
Compressor 4	$Z_{\mathrm{Com4}} = 10167.5(\dot{W}_{\mathrm{Com4}})^{0.46}$	$\dot{C}_{21} + \dot{C}_{\mathrm{C4}} + \dot{Z}_{\mathrm{Com4}} = \dot{C}_{22}$	-
Ammonia Reactor	$Z_{\mathrm{Reac}} = 283(\dot{Q}_{\mathrm{Reac}})$	$\dot{C}_{22} + \dot{C}_{\mathrm{Q}} + \dot{C}_4 + \dot{Z}_{\mathrm{Reac}} = \dot{C}_{23} + \dot{C}_5$	
Condenser 2	$Z_{\mathrm{Cond2}} = 2143(A_{\mathrm{Cond2}})^{0.514}$	$\dot{C}_{23} + \dot{C}_{36} + \dot{Z}_{\mathrm{COND2}} = \dot{C}_{24} + \dot{C}_{25} + \dot{C}_{37}$	$c_{23} = c_{24}$ $c_{23} = c_{25}$
PEM-HE	$Z_{\mathrm{PEM-HE}} = 130(\frac{A_{\mathrm{PEM-HE}}}{0.093})^{0.78}$	$\dot{C}_{26} + \dot{C}_{22} + \dot{Z}_{\mathrm{PEM-HE}} = \dot{C}_{27} + \dot{C}_{23}$	$c_{12} = c_{13}$
PEM Electrolyzer	$Z_{\mathrm{PEM-Elec}} = 3600 \times 24 \times 4 \times \dot{m}_{PEM-H2}$	$\dot{C}_{27} + \dot{C}_{\mathrm{W\_Net}} + \dot{Z}_{\mathrm{PEM-Elec}} = \dot{C}_{28} + \dot{C}_{29}$	-

Finally, the system sum unit product cost (SUCP) based on recognized cost and exergetic rates for the recommended cogeneration energy system products can be expressed as follows:

$$SUCP = \frac{\dot{C}_{H2} + \dot{C}_{NH3} + \dot{C}_{tur}}{\dot{E}_{PEM} + \dot{E}_{NH3reactor} + \dot{W}_{Net}} \quad (19)$$

Figure 2 plots the flowchart of the techno-economic modeling in this work.

3. Verification of the developed model

To certify the ammonia synthesis unit modeling, the fluctuation of the mole fraction of ammonia with the reactor is compared with the results in the literature [35], as can be seen in Fig. 3.

There is an acceptable agreement between the simulated ammonia synthesis predictions in the current study and the literature [35].

In Table 5, the model development validation in the present work and different related works [36] [37] are given. It is seen that there is less than a 5% error between the results of the current work and the considered literature.

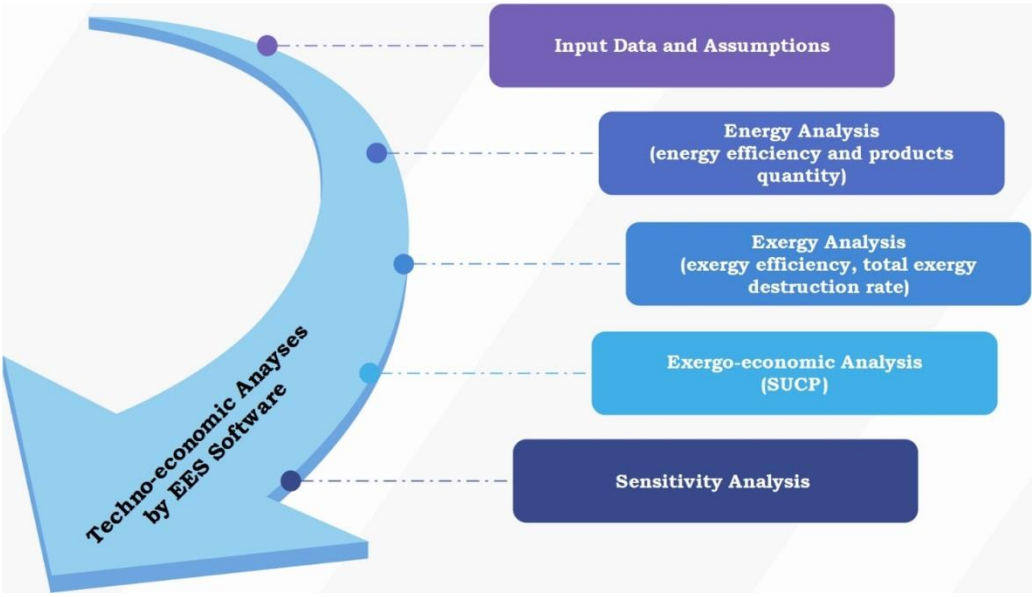

Fig. 2. The techno-economic modeling process

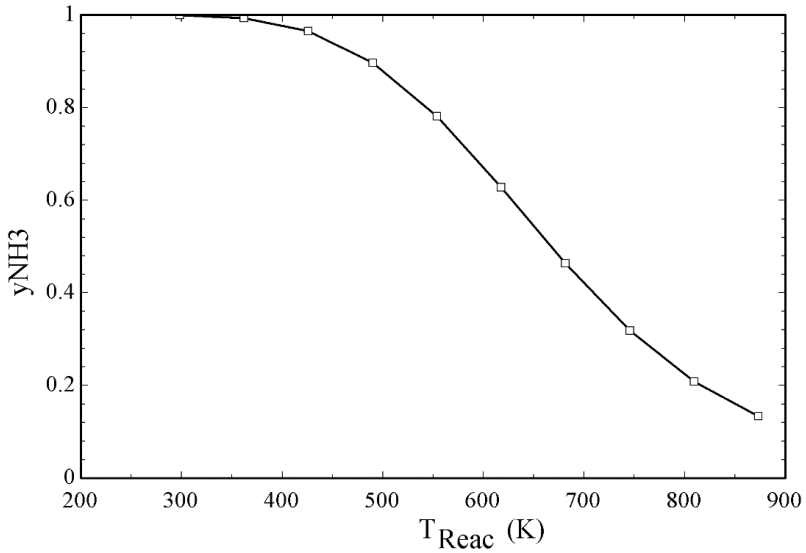

Fig. 3. Verification of the ammonia synthesis unit

Table 5. Model validation between present works with Ref

Cycle	Parameter	Present work	Reference	Relative error (%)
(a)			Sun et al. [36]	
KCS	Vapor generator load $\dot{Q}_{VG}(kW)$	3964	3905	1.52
	Net power output $\dot{W}_{NET}(kW)$	286.3	285.6	0.24
	Ammonia concentration at turbine outlet $X_{TUR}(\%)$	99.97	99.97	0
	First-law efficiency $\eta_I(\%)$	7.22	7.17	0.69
(b)			Ahmadi et al. [37]	
PEM	Electrolyzer temperature ($^{\circ}$C)	80	80	0
	Water primary temperature ($^{\circ}$C)	25	25	0
	Water pressure (kPa)	101	101	0
	Net output power (kW)	101	101.96	0.5
	Energy efficiency (%)	3.75	3.6	4
	Exergy efficiency (%)	23.1	22.7	1.7
	Electrolyzer exergy efficiency (%)	57.15	56.34	1.4
	Hydrogen production rate (kg/h)	1.197	1.2	0.2

4. Result and discussions

The modeling results for energy, exergy, and exergoeconomic provide a better perspective on the overall thermal efficiency, exegetic efficiency, hydrogen and ammonia production rates, and SUCP of the system. Also, the thermodynamic properties of each state of the system were tabulated in Table 6.

Table 6. Thermodynamic properties of the streams for the system.

State	Fluid	T (K)	P (bar)	h $(kJ.km^{-1})$	s $(kJ.km^{-1}.K^{-1})$	$\dot{m}$ $(kg.S^{-1})$
1	NH_3-H_2O	413.2	20	607.5	2.203	42
2	NH_3-H_2O	413.2	20	1710	5.147	5.601
3	NH_3-H_2O	413.2	20	437.7	1.75	36.4
4	Water	333.4	20	78.41	0.7852	36.4
5	NH_3-H_2O	392.2	20	317.5	1.487	42
6	NH_3-H_2O	348.5	3.197	1453	5.278	5.601
7	NH_3-H_2O	338.5	3.197	261.7	1.391	42
8	NH_3-H_2O	323.2	3.197	3.762	0.6145	42
9	NH_3-H_2O	323.4	20	6.056	0.6155	42
10	NH_3-H_2O	333.7	3.197	78.41	0.7909	36.4
11	Steam	433.2	9	12175	35	40
12	Steam	393.2	9	9085	27.51	40
13	Hydrogen	298.2	1.013	0	130.6	1.512
14	Nitrogen	298.2	1.013	0	191.5	7.003
15	Reactants	298.2	1.013	0	145.8	8.515
16	Reactants	860	10.06	16583	157.9	8.515
17	Reactants	298.2	10.06	0	126.7	8.515
18	Reactants	636.9	31.73	9905	139.3	8.515
19	Reactants	298.2	31.73	0	117.2	8.515
20	Reactants	548.2	56.32	7293	130.1	8.515
21	Reactants	298.2	56.32	0	112.4	8.515
22	Reactants	548.2	100	7293	125.4	8.515
23	Products	548.2	100	-19646	169.9	11.55
24	Ammonia	548.2	100	-36064	178.4	6.528
25	Hydrogen	298.2	100	0	92.38	0.1176
26	Water	298	1	1877	6.572	0.01597
27	Water	353	1	6023	19.34	0.01597
28	Hydrogen	353	1	9516	112.6	0.001788
29	Oxygen	353	1	1612	5.074	0.01417
30	Water	298.2	1	1889	6.61	7.188
31	Water	318.2	1	3396	11.5	7.188

A parametric study should be conducted to check for the effect of the decision variables to glimpse the function of the exemplified plant, the clear values of all influential variables which are the results of the simulation of the plant are delivered in Table 7. This Table provides a detailed scene of the modeling development of the plant. Thermal efficiency, exergy efficiency, ammonia synthesis thermal efficiency, SUCP, as well as the total exergy destruction rate of the plant, is calculated to be 50.47%, 51.41%, 48.86%, 638.3 $/GJ, and 89897 kW, successively. In addition, the provided hydrogen and ammonia rates by the cogeneration plant are 6.438 kg/h and 6.528 kg/s, respectively.

Likewise, the exergy and exergoeconomic values for different components are given in Table 8. The maximum destroyed exergy rate belongs to compressor1, thus more refinement must be devoted to this element since the maximum irreversibility and inefficiencies are affiliated with it. The ammonia synthesis reactor followed by compressr2 has the highest exergy destruction rate. From the exergoeconomic aspect, the maximum exergy destruction cost rate is related to the ammonia synthesis reactor guiding that the exergy destruction of this unit should be diminished.

Sensitivity analysis shows that the reactor pressure is the most affecting parameter. Fig. 4 depicts the reactor pressure versus efficiencies, SUCP, and provided ammonia rates of the system. Increasing P_{Reac} from 50 to 400 bar has increased energy efficiency and ammonia production. The reason for this trend is that y_{NH3} increases, which causes an increase in the mass flow rate of produced ammonia, which ultimately increases energy efficiency. Also, it can be seen that with the increase in reactor pressure due to the increase in the work of the compressors, the exergy efficiency and the SUCP of the system decrease owing to the increase in the reactor output exergy and decrease in $\dot{C}_{Tur}$.

Table 7. Performance parameters resulted from the evaluation of the proposed system.

Performance parameter	value	Performance parameter	value
Ammonia Reactor heat load, $\dot{Q}_{\mathrm{Ammo-Reac}}$ (kW)	12180	Cost per exergy unit of Turbine power, c_{TUR} ($/GJ)	182.4
Inter cooling 1 duty, $\dot{Q}_{\mathrm{Int-cool1}}$ (kW)	2801	Hydrogen production rate, $\dot{m}_{\mathrm{Hydrogen}}$ (kg/h)	6.438
Inter cooling 2 duty, $\dot{Q}_{\mathrm{Int-cool2}}$ (kW)	2070	PEM thermal efficiency, $\eta_{\mathrm{th,PEM}}$ (%)	2.122
Inter cooling 3 duty, $\dot{Q}_{\mathrm{Int-cool3}}$ (kW)	1780	PEM exergy efficiency, $\eta_{\mathrm{ex,PEM}}$ (%)	15.47
Condenser 1 load, $\dot{Q}_{\mathrm{Cond1}}$ (kW)	10833	PEM exergy destruction, $\dot{E}_{D,PEm}$ (kW)	1148
Condenser 2 load, $\dot{Q}_{\mathrm{Cond2}}$ (kW)	13239	Cost per exergy unit of hydrogen production, $c_{Hydrogen}$ ($/GJ)	1146
Compressor 1 power, $\dot{W}_{\mathrm{Com1}}$ (kW)	33461	Ammonia production rate, $\dot{m}_{\mathrm{NH3}}$ (kg/s)	6.528
Compressor 2 power, $\dot{W}_{\mathrm{Com2}}$ (kW)	14308	Ammonia synthesis thermal efficiency, $\eta_{\mathrm{th-Syn}}$ (%)	48.86
Compressor 3 power, $\dot{W}_{\mathrm{Com3}}$ (kW)	6656	Ammonia Synthesis exergy efficiency, $\eta_{\mathrm{ex-Syn}}$ (%)	50.23
Compressor 4 power, $\dot{W}_{\mathrm{Com4}}$ (kW)	6656	Ammonia Synthesis exergy destruction rate, $\dot{E}_{\mathrm{D-Syn}}$ (kW)	55989
Turbine power, $\dot{W}_{\mathrm{TUR}}$ (kW)	1443	Cost per exergy unit of Ammonia production, c_{Syn} ($/GJ)	655.3
Pump power, $\dot{W}_{\mathrm{PUM}}$ (kW)	96.38	System thermal efficiency, $\eta_{\mathrm{th-Sys}}$ (%)	50.47
KSC thermal efficiency, $\eta_{\mathrm{th,KSC}}$ (%)	11.06	System exergy efficiency, $\eta_{\mathrm{ex-Sys}}$ (%)	51.41
KSC exergy efficiency, $\eta_{\mathrm{ex,KSC}}$ (%)	24.24	System exergy destruction rate, $\dot{E}_{\mathrm{D}}$ (kW)	89797
KSC exergy destruction, $\dot{E}_{D,KSC}$ (kW)	32659	Total SUCP of the system, $SUCP$ ($/GJ)	638.3

Table 8. Component cost rates and exergoeconomic factors for the proposed systems.

Components	$\dot{E}x_{D,k}(kW)$	$c_{F,k}(\frac{\$}{GJ})$	$c_{P,k}(\frac{\$}{GJ})$	$\dot{C}_{D,k}(\frac{\$}{s})$	$\dot{Z}_k(\frac{\$}{s})$
KSC-Turbine	219.2	66.96	182.4	52.85	151938
Separator	70.18	66.13	66.96	16.71	0
Mixer	53.36	68.08	68.08	13.63	0
Regenerator	450.2	66.96	97.04	108.5	34877
Condenser 1	765.2	68.08	275.6	187.5	20098
Pump	96.38	182.4	443.1	8.754	19223
Compressor 1	20475	0	84.43	0	259829
Inter cooling 1	5464	63.4	251.5	1247	2150
Compressor 2	8167	133.9	340.7	3938	175778
Inter cooling 2	2195	1475	4414	11654	2246
Compressor 3	3233	259.2	611.3	3017	123613
Inter cooling 3	1188	3292	8106	14080	2337
Compressor 4	6656	259.2	611.3	3017	123613
Reactor	10386	550.2	1133	20570	730476
Condenser 2	1650	187.9	567	1116	11056
PEM-HE	10.57	1.3	37.23	0.049	180.9
PEM Electrolyzer	1138	181.8	1117	744.8	19.05

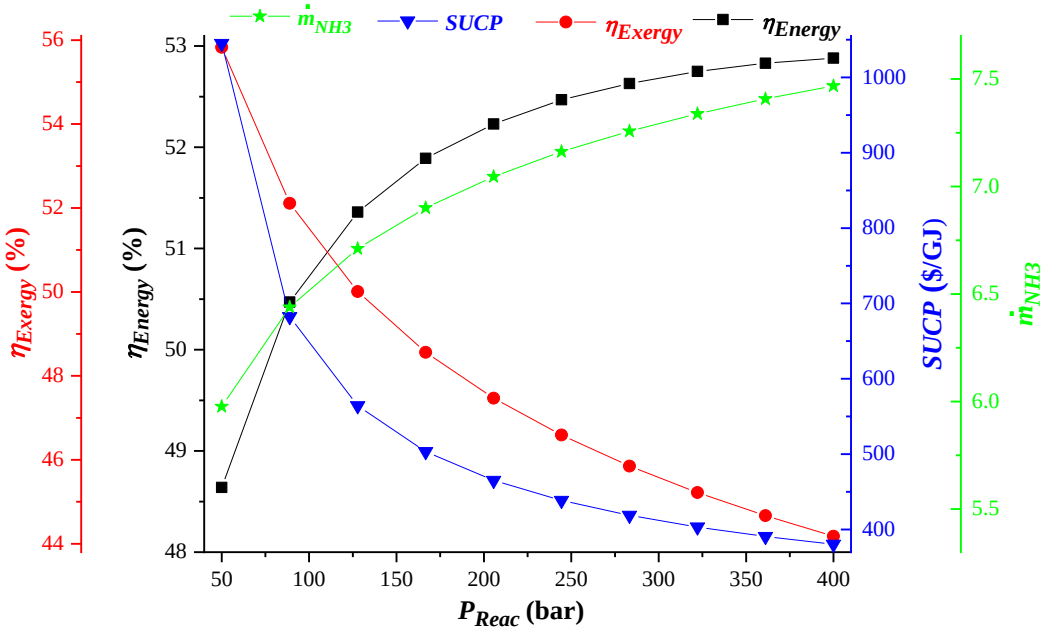

Fig. 4. The effect of reactor pressure on the energy and exergy efficiencies, NH_3 production rate, and SUCP

Figure 5 shows the reactor temperature effect on the efficiencies, SUCP, and provided ammonia rates of the system. The increase of T_{Reac} from 450 K to 650 K has caused a decrease in energy and exergy efficiencies and the amount of ammonia production. The reason for this trend is that y_{NH3} decreases, which causes a decrease in the mass flow rate of produced ammonia and ultimately causes a decrease in yields. In addition, the SUCP of the system has increased due to the increase in the heat given to the cycle and the subsequent increase in the cost of power generation in the turbine ($\dot{C}_{Tur}$).

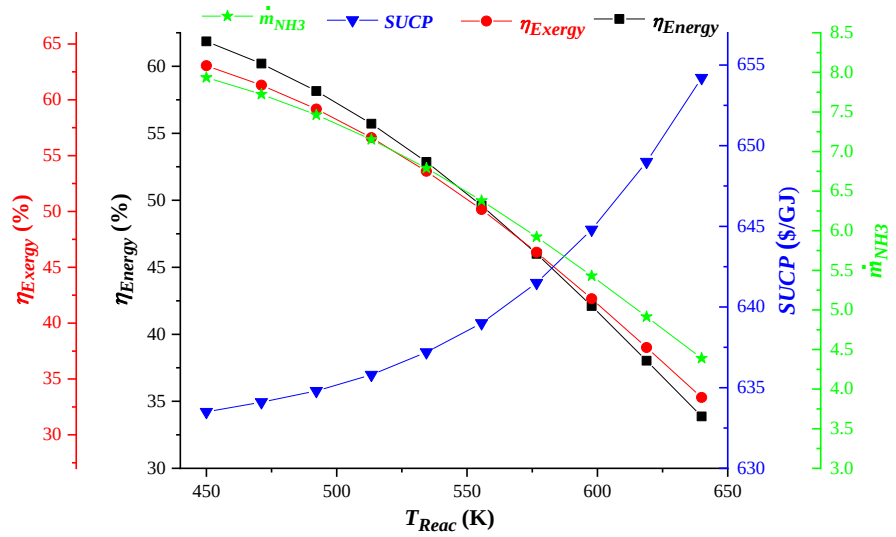

Fig. 5. The effect of reactor temperature on the energy and exergy efficiencies, NH_3 production rate, and SUCP

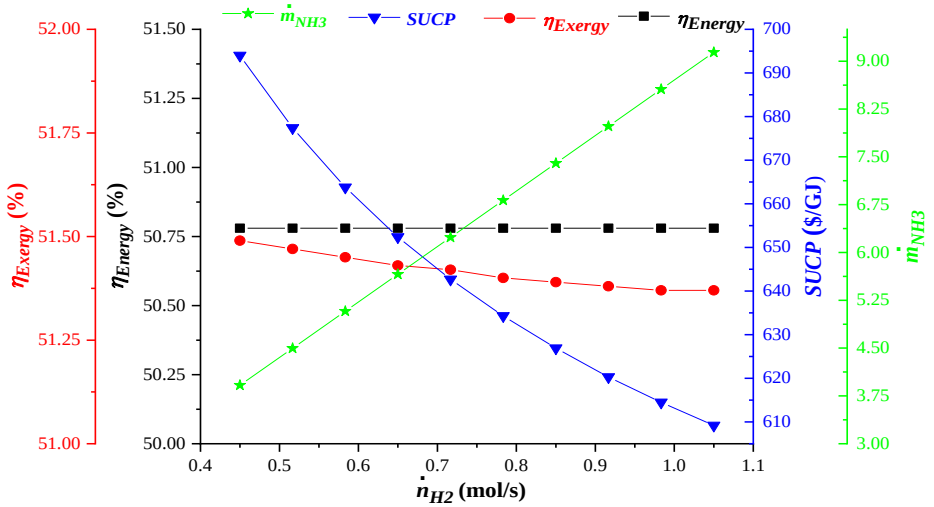

Fig. 6. The effect of input hydrogen molar ratio on the energy and exergy efficiencies, NH_3 production rate, and SUCP

Figure 6 illustrates the variations of input hydrogen molar ratio with efficiencies, SUCP, and provided ammonia rates of the system. It can be seen that with incre2 from $\dot{n}_{H2}$ from 0.45 to 1.05 mol/s, the energy efficiency remains constant. Since y_{NH3} has remained constant in the reaction and only had an increase in the mass flow rate of ammonia, which is equal to the increase in mass flow rate at the reactor inlet, so the energy efficiency has remained constant. In addition, the SUCP of the system and the exergy efficiency have also decreased slightly due to the very low increase in the exergy of the reactor.

Figure 7 shows the ratio of hydrogen to nitrogen with efficiencies, SUCP, and provided ammonia rates of the system. It can be seen that by increasing the ratio of hydrogen to nitrogen up to 3.5, the energy efficiency increases, and consequently decreases, so it can be said that the number 3.5 is the optimal ratio of hydrogen to nitrogen. In addition, ammonia production and consequently the exergy efficiency increase. In addition, the SUCP of the system is reduced due to the higher production of ammonia in constant thermodynamic conditions.

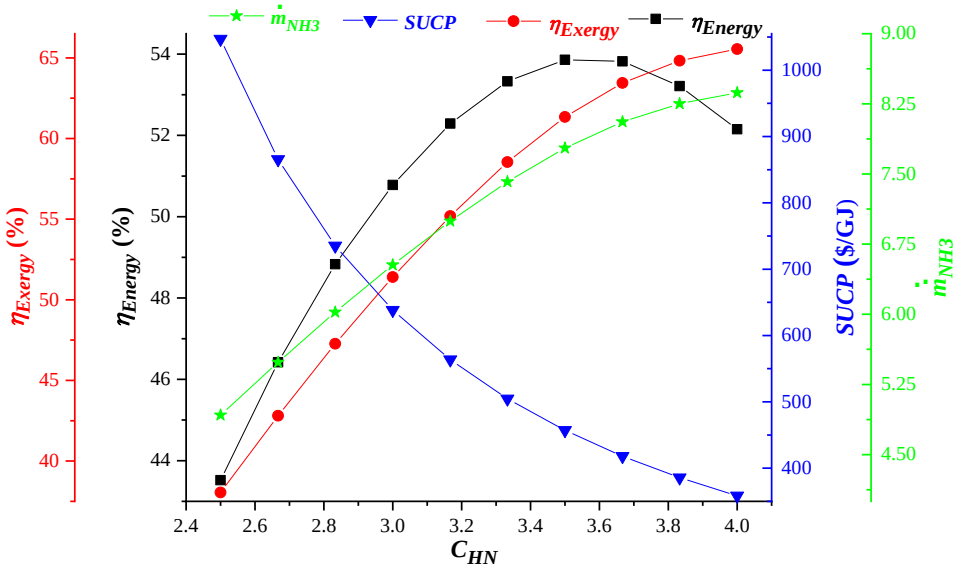

Fig. 7. The effect of the ratio of hydrogen to nitrogen on the energy and exergy efficiencies, NH_3 production rate, and SUCP

5. Conclusions

In the current study, a new cogeneration energy plant for useful commodities such as ammonia, and hydrogen as well as power production is analyzed based on the first and second laws of thermodynamics. Moreover, the plant's sum unit cost of products (SUCP) is studied. To achieve higher energy and exergy efficiencies and the lowest SUCP and rate of total destructed exergy, the plant has been satisfied with the attentive configuration of the modified Rankine cycle, ammonia synthesis reactor, as well as PEM electrolyzer equipment. Likewise, to investigate the significance of the pivotal input configuration variables on the ammonia production rate, and economic performance criteria of the offered cogeneration energy system, an exhaustive sensitivity breakdown is conducted and discussed in detail. Besides, the developed model validation has been done using previous related works in the literature, with a less than 5% error. In the sensitivity analysis, several principal variables containing the synthesis reactor's pressure, and its temperature, the input hydrogen molar ratio, and the hydrogen to nitrogen molar ratio are deemed for fluctuations. Some noteworthy concluding attributes of the current work are stated as follows:

- The thermal efficiency, exergy efficiency, ammonia synthesis thermal efficiency, SUCP, as well as the total exergy destruction rate of the plant are calculated as 50.47%, 51.41%, 48.86%, 638.3 $/GJ, and 89897 kW, respectively.
- The provided hydrogen and ammonia rates by the cogeneration plant are 6.438 kg/h and 6.528 kg/s.
- The maximum exergy destruction is associated with compressor1.
- The maximum exergy destruction cost rate is related to the ammonia synthesis reactor.
- The synthesis reaction temperature deviation on the overall efficiencies and ammonia production rate of the offered plant has a negative mark while by synthesis reaction pressure changes, ammonia production rate and energy efficiency have a rising trend.
- Increasing the input hydrogen molar ratio has a positive mark on the economic performance and rate of the provided ammonia by the plant.
- By changing the hydrogen-to-nitrogen molar ratio economic operation criteria have a descending tendency.

References

[1] Gielen, Dolf, Ricardo Gorini, Nicholas Wagner, Rodrigo Leme, Laura Gutierrez, Gayathri Prakash, Elisa Asmelash, Luis Janeiro, Giacomo Gallina, and Guilia Vale, Global energy transformation: a roadmap to 2050. 2019.

[2] Ghaebi, Hadi, Behzad Farhang, Hadi Rostamzadeh, and Towhid Parikhani, Energy, exergy, economic and environmental (4E) analysis of using city gate station (CGS) heater waste for power and hydrogen production: A comparative study. International Journal of Hydrogen Energy, 2018. 43(3): p. 1855-1874.

[3] Hasanzade, Maryam, Milad Feili, and Hadi Ghaebi, Development and analysis of a novel multi-generation system fueled by biogas with smart heat recovery.

[4] Bezaatpour, Javad, Hamed Ghiasirad, Mojtaba Bezaatpour, and Hadi Ghaebi, Towards optimal design of photovoltaic/thermal facades: Module-based assessment of thermo-electrical performance, exergy efficiency and wind loads. Applied Energy, 2022. 325: p. 119785.

[5] Feili, Milad, Maryam Hasanzadeh, Hadi Ghaebi, and Ebrahim Abdi Aghdam, Comprehensive analysis of a novel cooling/electricity cogeneration system driven by the waste heat of a marine diesel engine. Energy Sources, Part A: Recovery, Utilization, and Environmental Effects, 2022. 44(3): p. 7331-7346.

[6] Feili, Milad, Hadi Rostamzadeh, and Hadi Ghaebi, Thermo-mechanical energy level approach integrated with exergoeconomic optimization for realistic cost evaluation of a novel micro-CCHP system. Renewable Energy, 2022. 190: p. 630-657.

[7] Akhoondi, Asieh, Hadi Ghaebi, Lakshmanan Karuppasamy, Mohammed M Rahman, and Panneerselvam Sathishkumar, Recent advances in hydrogen production using MXenes-based metal sulfide photocatalysts. Synthesis and Sintering, 2022. 2(1): p. 37-54.

[8] Ghaebi, Hadi, Elahe Soleimani, Saeed Ghavami Gargari, and Shahin Basiri, Energy, Exergy and Thermoeconomic Analysis of the Novel Combined Cycle of Solid Oxide Fuel Cell (SOFC) and Biogas Steam Reforming (BSR) for Cogeneration Power and Hydrogen. Amirkabir Journal of Mechanical Engineering, 2022. 54(1): p. 10-10.

[9] Hashemian, Nasim, Alireza Noorpoor, and Majid Amidpour, A Biomass Assisted Solar-Based Multi-generation Plant with Hydrogen and Freshwater Production: Sustainability, Advanced Exergy and Advanced Exergo-Economic Assessments, in Synergy Development in Renewables Assisted Multi-carrier Systems. 2022, Springer. p. 107-125.

[10] Chitgar, Nazanin, and Mohammad Ali Emadi, Development and exergoeconomic evaluation of a SOFC-GT driven multi-generation system to supply residential demands: Electricity, fresh water and hydrogen. International Journal of Hydrogen Energy, 2021. 46(34): p. 17932-17954.

[11] Musharavati, Farayi, Shoaib Khanmohammadi, and Amirhossein Pakseresht, Proposed a new geothermal based poly-generation energy system including Kalina cycle, reverse osmosis desalination, elecrolyzer amplified with thermoelectric: 3E analysis and optimization. Applied Thermal Engineering, 2021. 187: p. 116596.

[12] Jabari, Farkhondeh, Hamidreza Arasteh, Alireza Sheikhi-Fini, Hadi Ghaebi, Mohammad-Bagher Bannae-Sharifian, Behnam Mohammadi-Ivatloo, and Mousa Mohammadpourfard, A biogas-steam combined cycle for sustainable development of industrial-scale water-power hybrid microgrids: design and optimal scheduling. Biofuels, Bioproducts and Biorefining, 2022. 16(1): p. 172-192.

[13] Soleymani, Elahe, Saeed Ghavami Gargari, and Hadi Ghaebi, Thermodynamic and thermoeconomic analysis of a novel power and hydrogen cogeneration cycle based on solid SOFC. Renewable Energy, 2021. 177: p. 495-518.

[14] Cao, Yan, Leonardus WW Mihardjo, Behzad Farhang, Hadi Ghaebi, and Towhid Parikhani, Development, assessment and comparison of three high-temperature

geothermal-driven configurations for power and hydrogen generation: Energy, exergy thermoeconomic and optimization. International Journal of Hydrogen Energy, 2020. 45(58): p. 34163-34184.

[15] Sadat, Seyed Mohammad Sattari, Hadi Ghaebi, and Arash Mirabdolah Lavasani, 4E analyses of an innovative polygeneration system based on SOFC. Renewable Energy, 2020. 156: p. 986-1007.

[16] Yilmaz, Fatih and Murat Ozturk, Design and modeling of an integrated combined plant with SOFC for hydrogen and ammonia generation. International Journal of Hydrogen Energy, 2022.

[17] Klein, SA, Engineering Equation Solver (EES) V9, F-chart software, Madison, USA. 2015.

[18] Cao, Yan, Hima Nikafshan Rad, Danial Hamedi Jamali, Nasim Hashemian, and Amir Ghasemi, A novel multi-objective spiral optimization algorithm for an innovative solar/biomass-based multi-generation energy system: 3E analyses, and optimization algorithms comparison. Energy Conversion and Management, 2020. 219: p. 112961.

[19] Heidarnejad, P., N. Hashemian, and A.R. Noorpoor, Multi Objective Exergy Based Optimization of a Solar Micro CHP System Based on Organic Rankine Cycle. Journal of Solar Energy Research, 2017. 2(2): p. 41-47.

[20] Ghaebi, Hadi, Towhid Parikhani, Hadi Rostamzadeh, and Behzad Farhang, Proposal and assessment of a novel geothermal combined cooling and power cycle based on Kalina and ejector refrigeration cycles. Applied Thermal Engineering, 2018. 130: p. 767-781.

[21] Hashemian, Nasim and Alireza. Noorpoor, A geothermal-biomass powered multi-generation plant with freshwater and hydrogen generation options: Thermo-economic-environmental appraisals and multi-criteria optimization. Renewable Energy, 2022.

[22] Noorpoor, Alireza, Parisa Heidarnejad, Nasim Hashemian, and Amir Ghasemi, A thermodynamic model for exergetic performance and optimization of a solar and biomass-fuelled multigeneration system. Energy Equipment and Systems, 2016. 4(2): p. 281-289.

[23] Deng, Xiangtian, Yi Zhang, and He Qi, Towards optimal HVAC control in non-stationary building environments combining active change detection and deep reinforcement learning. Building and environment, 2022. 211: p. 108680.

[24] Parikhani, Towhid, Towhid Gholizadeh, Hadi Ghaebi, Seyed Mohammad Sattari Sadat, and Mehrdad Sarabi, Exergoeconomic optimization of a novel multigeneration system driven by geothermal heat source and liquefied natural gas cold energy recovery. Journal of cleaner production, 2019. 209: p. 550-571.

[25] Noorpoor, AR, D Hamedi, and N Hashemian, Optimization of parabolic trough solar collectors integrated with two stage Rankine cycle. Journal of Solar Energy Research, 2017. 2(2): p. 61-66.

[26] Bejan, Adrian, George Tsatsaronis, and Michael J Moran, Thermal design and optimization. 1995: John Wiley & Sons.

[27] Kordlar, M Akbari and SMS Mahmoudi, Exergeoconomic analysis and optimization of a novel cogeneration system producing power and refrigeration. Energy Conversion and Management, 2017. 134: p. 208-220.

[28] Hashemian, Nasim and Alireza Noorpoor, Optimization and multi-aspect evaluation of a solar/biomass-powered multi-generation plant with an integrated thermoelectric generator unit. Sustainable Energy Technologies and Assessments, 2023. 56: p. 102998.

[29] Habibollahzade, Ali, Ehsan Houshfar, Pouria Ahmadi, Amirmohammad Behzadi, and Ehsan Gholamian, Exergoeconomic assessment and multi-objective optimization of a solar chimney integrated with waste-to-energy. Solar Energy, 2018. 176: p. 30-41.

[30] Yin, Jiqiang, Zeting Yu, Chenghui Zhang, Minli Tian, and Jitian Han, Thermodynamic analysis and multi-objective optimization of a novel power/cooling cogeneration system for low-grade heat sources. Energy Conversion and Management, 2018. 166: p. 64-73.

[31] Habibollahzade, Ali, Ehsan Gholamian, Pouria Ahmadi, and Amirmohammad

Behzadi, Multi-criteria optimization of an integrated energy system with thermoelectric generator, parabolic trough solar collector and electrolysis for hydrogen production. International journal of hydrogen energy, 2018. 43(31): p. 14140-14157.

[32] Ghaebi, Hadi, Behzad Farhang, Towhid Parikhani, and Hadi Rostamzadeh, Energy, exergy and exergoeconomic analysis of a cogeneration system for power and hydrogen production purpose based on TRR method and using low grade geothermal source. Geothermics, 2018. 71: p. 132-145.

[33] Ghaebi, Hadi, Towhid Parikhani, Hadi Rostamzadeh, and Behzad Farhang, Thermodynamic and thermoeconomic analysis and optimization of a novel combined cooling and power (CCP) cycle by integrating of ejector refrigeration and Kalina cycles. Energy, 2017. 139: p. 262-276.

[34] Lavasani, Arash Mirabdolah and Hadi Ghaebi, Economic and thermodynamic evaluation of a new solid oxide fuel cell based polygeneration system. Energy, 2019. 175: p. 515-533.

[35] Saxena, Abhishek, Sanford Klein and Gregory Nellis: Thermodynamics: Cambridge University Press, Printed in the United States of America, 2012, 1102 pp, ISBN: 978-0-521-19570-6. Journal of Thermal Analysis and Calorimetry, 2012. 110(1): p. 509-511.

[36] Sun, Xiufu, Ming Chen, Søren Højgaard Jensen, Sune Dalgaard Ebbesen, Christopher Graves, and Mogens Mogensen, Thermodynamic analysis of synthetic hydrocarbon fuel production in pressurized solid oxide electrolysis cells. International journal of hydrogen energy, 2012. 37(22): p. 17101-17110.

[37] Ahmadi, Pouria, Ibrahim Dincer, and Marc A Rosen, Energy and exergy analyses of hydrogen production via solar-boosted ocean thermal energy conversion and PEM electrolysis. International Journal of Hydrogen Energy, 2013. 38(4): p. 1795-1805.

[38] Hashemian, Nasim and Alireza Noorpoor, Assessment and multi-criteria optimization of a solar and biomass-based multi-generation system: Thermodynamic, exergoeconomic and exergoenvironmental aspects. Energy Conversion and Management, 2019. 195: p. 788-797.

[39] Ni, Meng, Michael KH Leung, and Dennis YC Leung, Energy and exergy analysis of hydrogen production by solid oxide steam electrolyzer plant. International journal of hydrogen energy, 2007. 32(18): p. 4648-4660.

[40] Hashemian, Nasim, Alireza Noorpoor, and Parisa Heidarnejad, Thermodynamic diagnosis of a novel solar-biomass based multi-generation system including potable water and hydrogen production. Energy Equipment and Systems, 2019. 7(1): p. 81-98.

[41] Esmaili, P, I Dincer, and GF Naterer, Energy and exergy analyses of electrolytic hydrogen production with molybdenum-oxo catalysts. International journal of hydrogen energy, 2012. 37(9): p. 7365-7372.

Appendix A

Appendix A presents the thermodynamic modeling method of the PEM electrolyzer. The water electrolysis process orders the following energy quantity [38]:

$$\Delta H = \Delta G + T\Delta S \tag{A.1}$$

ΔG is known as Gibbs free energy, whereas TΔS is the demanded thermal energy. Calculation of the mass flow rate of hydrogen coming out of an electrolysis process is done by utilizing the subsequent equation [39]:

$$\dot{m}_{H_2O,reacted} = \dot{m}_{H_2,out} = \frac{J}{2F} \tag{A.2}$$

F denotes the Faraday constant, and J signifies the density of the fluid.

In the PEM electrolyzer, hydrogen is provided by employing electricity that is generated by the system or external source [40]:

$$E_{power} = JV \tag{A.3}$$

The total voltage of the PEM electrolyzer, in this case, represents by V:

$$V_{total} = V_0 + V_{act,a} + V_{act,c} + V_{ohm} \tag{A.4}$$

Here V_0, $V_{act,\,a}$, $V_{act,c}$, and V_{ohm} signify the reversible potential, activation overpotential in the anode side, activation overpotential in the cathode side, and electrolyte ohmic overpotential, respectively. The anode and cathode are shown by the subscripts a and c, each. Reversible potential shows itself as [39]:

$$V_0 = 1.23 - 85\times10^{-5}\left(T_{PEM} - 298.15\right) \tag{A.5}$$

Moreover, the membrane's local ionic conductivity can be written that way [39]:

$$\sigma\left(\lambda(x)\right) = exp\left(127\times\left(\frac{1}{303}-\frac{1}{T}\right)\right).\left(0.514\times\lambda(x) - 0.33\right) \tag{A.6}$$

In this equation, x denotes the depth of the membrane from the cathode side to the membrane and $\lambda(x)$ refers to the content of water at a location of x. $\lambda(x)$ may be calculated as:

$$\lambda(x) = \lambda_{ca} + \left(\lambda_{an} - \lambda_{ca}\right)\frac{x}{l} \tag{A.7}$$

Here, l represents the thickness of the membrane, and λ_{an} and λ_{ca} denote water contents at the anode side and cathode side of the membrane interface, respectively.

Besides, the total ohmic resistance may be written as [38]:

$$R_{PEM} = \int_0^L \frac{dx}{\sigma\left(\lambda(x)\right)} \tag{A.8}$$

Ohmic overpotential can be computed relying on the Ohmic's Law as below [38]:

$$\eta_{ohm} = JR_{PEM} \tag{A.9}$$

To calculate electrode activity the activation overpotential is employed [39]:

$$\eta_{act,i} = \frac{RT}{F} ln\left(\frac{J}{2J_{0,i}} + \sqrt{\left(\frac{J}{2J_{0,i}}\right)^2 + 1}\right) = \frac{RT}{F}\sinh^{-1}\left(\frac{J}{2J_{0,i}}\right) \tag{A.10}$$

$J_{0,i}$ refers to the density of the exchange fluid and is computed as [41]:

$$J_{0,i} = J_i^{ref} exp\left(-\frac{E_{act,i}}{RT}\right) \tag{A.11}$$

where J_i^{ref} exists as a pre-exponential factor and $E_{act,i}$ signifies the activation energy for the anode side and cathode side.

Declaration of the competing interest

The authors declare that they have no known conflict of interest.